IEEE Access
Multidisciplinary | Rapid Review | Open Access Journal

Received March 26, 2021, accepted April 6, 2021, date of publication April 9, 2021, date of current version April 27, 2021.

Digital Object Identifier 10.1109/ACCESS.2021.3072197

Dynamic Properties Analysis of a New Kind of Inter-Connected Hydro-Pneumatic Strut

RUIHONG LI, FAN YANG, DEZHAO LIN, CHENGHONG LI, HONGWEI CHEN, WENBO QIAN, SHENG JIA, AND FENG ZHAO

College of Mechanical Engineering and Automation, Huaqiao University, Xiamen 361021, China

Corresponding author: Fan Yang (xmyf@hotmail.com)

This work was supported in part by the National Natural Science Foundation of China (NSFC) under Grant 61733006 and Grant U1813201.

ABSTRACT The dynamic properties of one kind of Inter-Connected Hydro-Pneumatic Struts (IC HPS), which is designed based on the developed double-gas-chamber compacted Hydro-Pneumatic Struts (HPS) integrating double inner gas chambers, will be investigated in this research. Comparing with the traditional IC HPS designs based on single gas chamber compacted HPS, the proposed IC HPS can postpone the force distortion, and then increase the working envelop, provide good stiffness performance and be stable in both In-Phase and Out-of-Phase working condition. The equation of motion of the proposed IC HPS will be derived firstly. And then based on the established dynamic model, the related simulating model will be established utilizing the AMEsim software, and the validity of the established simulating model will be verified on the basis of experimental data and available literatures. The validity and performance of the proposed IC HPS will be verified and investigated through comprehensive comparison with traditional IC HPS designs. Finally, the detailed sensitivity analysis of the essential design parameter of the proposed IC HPS will be presented to illustrate the advantage of the proposed IC HPS design.

INDEX TERMS Double-gas-chamber compacted Hydro-Pneumatic Struts, dynamic properties, sensitivity analysis.

I. INTRODUCTION

Vehicle suspension, as one of the most important parts in the vehicle to solve the conflict between ride comfort and vehicle handling [1], has increasingly development in recent years. To meet the requirement of large variation in operating loads and condition in practical applications, the semi-active/active suspension system with the properties of controllable stiffness/damping and working simultaneously [2], such as the Magneto-Rheological (MR) dampers, has been proposed [3]. However, high operating cost restrict this kind of semi-active/active suspension system to be widely accepted in practical applications [4]–[6]. The Hydraulically Interconnected Suspension (HIS) system is the other kinds of device to balance the ride and handling performance of vehicles [7]–[10], and has the potential to provide better suspension performance through semi-active/active control methodologies [11]–[13], comparing with the traditional mechanically interconnected suspension system, for example the anti-roll bar [14]. Recently, HIS has been popularly investigated and applied on Heavy duty Vehicles.

The associate editor coordinating the review of this manuscript and approving it for publication was Shihong Ding.

Most of research on HIS is based on the Hydro-pneumatic Strut (HPS) with external gas chamber [14]. Obviously, sometimes this kind of design cannot satisfy the installation space requirement. Wu [15] proposed one type of compacted HPS design, which integrated an inner air chamber separated with the hydraulic chamber through a floating piston in the rod section, as illustrated in Figure 1 (b) for single strut, and introduced the IC HPS design based on no orifices between the main and annual hydraulic chambers, as illustrated in Figure 1 (a). Cao *et al.* [16]–[19] extended the research work regarding the IC HPS design presented by Wu [15] through considering the fluid compressibility, and presented a set of research work focusing on the anti-roll and anti-pitch properties, handling performance and ride comfort. Guo *et al.* [20] modified the HPS design methodology presented by Wu [15] through changing the floating piston with an air bag, and also presented the investigation of IC HPS working condition. Here, it should be noted that the above research work on compacted HPS and its IC HPS are all based on numerical analysis, and lack of the experimental validation. Recently, Jiao *et al.* [21] studied the effect of temperature through the parametric modeling on this type of HPS. Zhang *et al.* [22] investigate the sensitivity analysis of this kind of HPS through

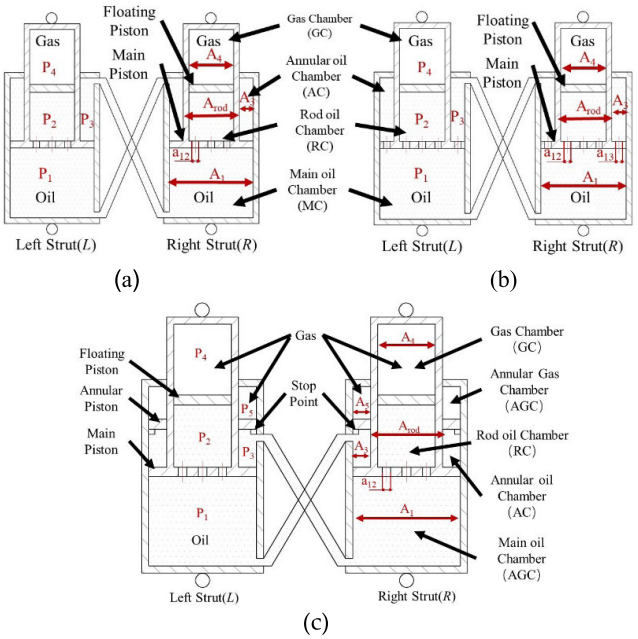

FIGURE 1. The structure diagram of three types of hydraulic interconnection hydro-pneumatic strut: (a) Type 1 IC HPS by Wu [15] (b) Type 2 IC HPS by Lin *et al.* [24] (c) Type 3 IC HPS Proposed in this paper.

the nonlinear mathematic model. Lin *et al.* [23] firstly investigated the dynamic properties of the single HPS design presented by Wu [15] and then its interconnection working condition, as illustrated in Figure 1 (b) [24]. Lin *et al.* [24] compared the dynamic properties of Type 2 IC HPS illustrated in Figure 1 (b) with those presented by Cao *et al.* [19], as illustrated in Figure 1 (a), through experimental set-up and the established AMEsim model. The results presented by Lin *et al.* [24] show that (1) For the IC HPS model presented by Wu [15] illustrated in Figure 1 (a), the phenomenon of output force distortion occurs under compression stroke in the In-Phase test, and it is easily to be totally block in the Out-of-Phase test. This is mainly related to the delay/block of the fluid flow in the interconnected pipes [24]; (2) For the model presented by Lin *et al.* [24], although the phenomenon of the output force distortion can be limited in small working range, it meets the small stiffness condition in the Out-of-Phase working condition which may be modified by changing the dimension of the size of orifices and/or connection pipes.

Considering the above, this research paper will propose a novel IC HPS design based on a developed double-gas-chamber HPS illustrated in Figure 1 (c) (Type 3 IC HPS) in which an extra air chamber will be installed in the annual chamber of HPS separated the fluid chamber through a floating piston as shown in Figure 1 (c). Fundamentally, this kind of design is focused on solving the phenomenon of the output force distortion and block of the design presented by Wu [15] illustrated in Figure 1 (a) (Type 1 IC HPS), and providing acceptably stiffness performance comparing with those introduced by Lin *et al.* [24] illustrated in Figure 1 (b) (Type 2 IC HPS). Firstly, the equation of motion of three kind of IC HPS designs will be derived. Then, the related dynamic models will be established based on the derived equation of motion through AMEsim software, and the validity of the established model will be verified through the comparison with available literatures and partial experimental data. Finally, extensive parameters analysis will be presented to illustrate the validity of the proposed IC HPS design and its advantage comparing with those presented by Wu [15], Cao *et al.* [16]–[19] and Lin *et al.* [24]. The result shows that (1) comparing with the design proposed by Wu [15], the added Annual Gas Chamber (AGC), working as an extra absorber, can postpone the flow fluid restriction (distortion), and then increase the working envelop in the In-Phase test signal; (2) comparing with the design proposed by Lin et al [24], the orifices between the main and annual fluid chamber in the proposed IC HPS have been cancelled, which can increase the system stiffness in the Out-of-Phase working condition; (3) the dynamic properties of the proposed IC-HPS can be easily modified through the pre-charging pressure in AGC in large working range.

II. MODELING OF INTERCONNECTION HYDRO-PNEUMATIC STRUTS

In this section, the equation of motion of three different kinds of IC HPS designs, as illustrated in Figure 1, will be established. The fundamental equation of motion is derived based on the relationship of force balance, volume conservation and the polytrophic process of gas.

A. MODELING OF TYPE 1 IC HPS

The first type of IC HPS, as shown in Figure 1 (a), is originally proposed by Wu [15], and its extensive investigation based on simulation have been presented by Cao *et al.* [19], and experimentally investigated by Lin *et al.* [24]. The key issue of this type of IC HPS design is that (1) Its single HPS integrates the gas accumulator in the rod section separating the hydraulic chamber through a floating piston; (2) No orifices exists between the Main oil Chamber (MC) and Annual oil Chamber (AC) in single HPS ;(3) The MC of HPS L (or R) is connected to the AC of HPS R (or L) through hydraulic pipes to establish the IC HPS system.

Ignoring the inertia force of the movement parts, the output forces F_i of struts i can be evaluated through:

$$F_i = P_{1i}A_1 - P_{3i}A_3 + F_{fi}sign(\dot{x}_i)(i = L, R) \qquad (1)$$

where P_{1i} and P_{3i} represent the pressure of MC and AC of strut i, respectively; A_1 and A_3 are the area of MC and AC, respectively; F_{fi} is the seal friction between piston rod and cylinder of strut i; $\dot{x}_i$ is the velocity of main piston, and downward direction is defined as positive direction. Here, it should be noted that as the main purpose of this paper is to propose and verify the validity of one type of novel IC HPS design, to simplify the expression, in this paper simple Coulomb damper model was utilized to describe the effect of the total output force associated with the friction on the floating piston(s), and its effect to the inner force balance,

which is related to the hydraulic pressure distribution, will be ignored.

Based on the principle of the volume conservation ignoring the fluid compressibility, the fluid flow can be expressed as:

$$Q_{1i} = -Q_{2i} - Q_{3j} \tag{2}$$
$$Q_{2i} = Q_{12i} \tag{3}$$
$$Q_{3j} = Q_{1i3j} \quad (i = L \text{ or } R;\ j = R \text{ or } L) \tag{4}$$

where Q_{1i} is the flow into the MC of strut i; Q_{2j} is the flow into the Rod oil Chamber (RC) of strut i; Q_{3j} is the flow into the AC of strut j; Q_{12i} is the flow from MC to RC; Q_{1i3j} is the flow from MC of strut i to AC of strut j through the hydraulic pipe.

Under the assumption of continuous flow, the flow of each strut can be obtained through the following equations:

$$Q_{1i} = -A_1 \cdot \dot{x}_i \tag{5}$$
$$Q_{2i} = A_4 \cdot \dot{x}_{4i} \tag{6}$$
$$Q_{3j} = A_3 \cdot \dot{x}_j \tag{7}$$

Therefore, the velocity of floating piston can be obtained from Equations (3)-(7):

$$\dot{x}_{4i} = \frac{A_1 \dot{x}_i - A_3 \dot{x}_j}{A_4} \tag{8}$$

where A_4 is the area of RC and Gas Chamber (GC) $\dot{x}_{4i}$ is the velocity of floating piston, and upward direction is defined as positive direction.

Based on the polytrophic process of ideal gas, the pressure (absolute) of GC can be expressed as:

$$P_{40i} \cdot V_{40i}^n = P_{4i} \cdot V_{4i}^n = constant \tag{9}$$
$$V_{4i} = V_{40i} - A_4 \cdot \Delta x_{4i} \tag{10}$$

where P_{40i} and P_{4i} represent the initial charging pressure (absolute) and working pressure (absolute) of GC, and their related volumes are defined as V_{40} and V_4, respectively. Δx_{4i} is the displacement of floating piston related to its initial position, which is associated to the V_{40}, and the upward direction is defined as positive; n is polytropic exponent.

The pressure of oil chamber can be expressed as:

$$P_{2i} = P_{4i} \tag{11}$$
$$P_{2i} = P_{1i} - \frac{Q_{12i}^2 \cdot \rho}{2(C_d \cdot a_{12i} \cdot n_{12i})^2} sign(\dot{x}) \tag{12}$$

where P_{1i} and P_{2i} are the pressure of MC and RC, respectively; ρ is the density of the oil; C_d is the flow coefficient; a_{12i} and n_{12i} are the area and number of the orifices between MC and RC, respectively.

The MC and AC of the left and right struts are only connected by a pipe and the pipe is too long to ignore its effect on the system, so the pressure of the two side of pipe that be affect by the long pipe must be considered. The basic formula of flow velocity of the long pipe can be expressed as:

$$v = \sqrt{\frac{2 \cdot D\,|\Delta P - 9.81 \cdot \rho \cdot L \cdot sin\theta|}{L \cdot \rho \cdot ff}} \tag{13}$$

where θ is the inclination of the pipe. Due to the effect of the inclination of the pipe is ignored in the experiment, the angle of the interconnection pipe assumed to be horizontal. The flow velocity in this experiment can be expressed as:

$$v_{1i3j} = \sqrt{\frac{2 \cdot D_{13} \cdot |\Delta P_{1i3j}|}{L_{13} \cdot \rho \cdot ff}} \tag{14}$$

where v_{1i3j} is the flow velocity from MC of strut i to AC of strut j through the interconnection pipe; D_{13} and L_{13} are the diameter and length of the pipe between MC of strut i and AC of strut j, respectively; ΔP_{1i3j} is the pressure drop between the MC of strut i and AC of strut j; ρ is the density of the oil and ff is the friction factor. The flow rate is then computed from the fluid velocity:

$$Q_{1i3j} = v_{1i3j} A_p \tag{15}$$

where A_p is the cross sectional area of the hydraulic pipe. As the main purpose of this paper is to investigate and verify the basic dynamic properties of these types of IC HPS, the compressibility of oil is neglected in the above equation.

B. MODELING OF TYPE 2 IC HPS

The second type of IC HPS was investigated by Lin *et al.* [24], in which orifices exist between MC and AC comparing with the strut of Type 1 IC HPS. Therefore, the flow distribution in Type 2 IC HPS will be re-arranged based on Equation (2) in Type 1 IC HPS as:

$$Q_{1i} = -Q_{2i} - (Q_{13i} + Q_{1i3j}) \tag{16}$$

and the fluid flow through the added orifices between MC and AC can be expressed as:

$$Q_{13i} = n_{13i} a_{13i} C_d \sqrt{\frac{2\,|\Delta P_{13i}|}{\rho}} sign(\dot{x}_i) \tag{17}$$

where Q_{13i} is the flow from MC to AC which is generated by the additional damping orifices; ΔP_{13i} is the pressure drop between MC and AC; a_{13i} and n_{13i} are the area and number of the orifices between MC and AC, respectively.

Therefore, the velocity of floating piston can be obtained from Equation (5),(6),(14)-(17):

$$\dot{x}_{4i} + \dot{x}_{4j} = \frac{A_2(\dot{x}_i + \dot{x}_j)}{A_4} \tag{18}$$

where A_2 is the area of the piston rod. Other equations related to Type 2 IC HPS are the same as those of the Type 1.

C. MODELING OF TYPE 3 IC HPS

The third type of IC HPS are shown in the Figure 1 (c), in which one extra gas chamber is arranged in the AC of its single HPS comparing with the single HPS of Type 1 IC HPS. The equation of flow rate is similar to Type 1 IC HPS, except flow distribution in Type 3 IC HPS will be re-arranged based on Equations (2) and (7) in Type 1 IC HPS as:

$$Q_{1i} = -Q_{2i} - Q_{3j} \tag{19}$$

$$Q_{3j} = Q_{1i3j} = A_3(\dot{x}_j + \dot{x}_{5j}) \tag{20}$$

where $\dot{x}_{5j}$ is the velocity of annular piston, and upward direction is defined as positive direction. Based on the polytrophic process of ideal gas, the pressure of AGC can be expressed as:

$$P_{50i} \cdot V_{50}^n = P_{5i} \cdot V_5^n = constant \tag{21}$$

$$V_{5i} = V_{50i} - A_5 \cdot \Delta x_{5i} \tag{22}$$

where P_{50i} and P_{5i} represents the initial charging pressure (absolute) and working pressure (absolute) of AGC, and their related volumes are defined as V_{50} and V_5, respectively; Δx_{5i} is the displacement of annular piston related to its initial position, which is associated to the V_{50}. Apart from the above, the other mathematical equations related to Type 3 IC HPS are the same as those of the Type 1.

III. EXPERIMENTAL AND TESTING SETUP

In this section, simulation models of three types of IC HPS will be established based on the derived equation of motion in the last section through AMEsim software. The validity of the established AMEsim model for Type 1 and 2 IC HPS will be verified through comparison with those presented by Lin *et al.* [24] and [23] under the same experimental setup and design parameters, which have been verified through experimental data. In order to keep the initial charging pressure in AGC, there is a ''stop point'' in the Type 3 IC HPS, as illustrated in Figure 1 (c), so the annular piston will be in stay at the ''stop point'' when the pressure in AGC lager than the working pressure of AC in working process without considering the inner effect of annular piston friction.

A. TESTING SETUP

The models of these three kinds of IC HPS are shown in the Figure 2, and Table 1 summarized all of the design parameters in the established simulation models. The testing setup in this paper consists of two parts: In-Phase test and Out-of-Phase test, as there are two typical excitation signals utilizing the performance of IC HPS system. The first series of simulation setup is the In-phase test, and can be expressed as:

$$x_i = Bcos\,(2\pi ft)\,(i = L, R) \tag{23}$$

where B and f are the amplitude and frequency of the harmonic excitation, respectively.

The second series of testing setup is the Out-of-Phase test, and can be expressed as:

$$x_L = Bcos(2\pi ft - \pi/2) \tag{24}$$

$$x_R = Bcos(2\pi ft + \pi/2) \tag{25}$$

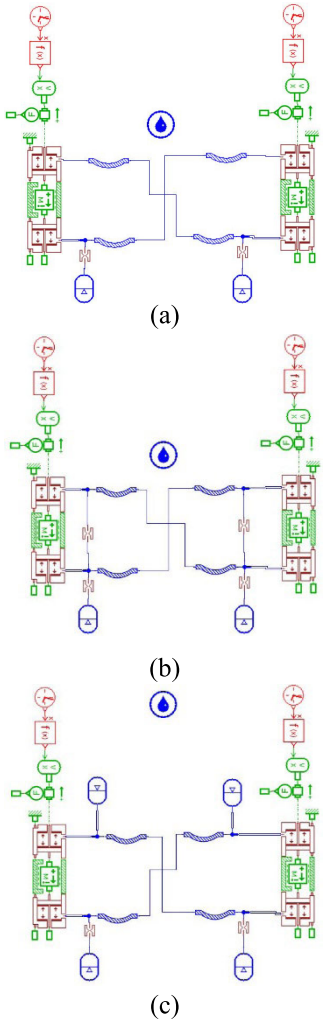

FIGURE 2. Simulation model based on the AMEsim software: (a) Type 1, (b) Type 2, and (c) Type 3.

Lin *et al.* [24] utilized two sets of excitation signals, as listed in Table 2, which will also be selected in this study, to verify the validity of the established AMEsim model for Type 1 and 2 IC HPS. Considering the fundamental structural design for Type 3 IC HPS, one can easily realize that under large initial charge pressure in the AGC, the Type 3 should be similar to Type 1 IC HPS, as the ''stop point'' will block the movement of annular piston and then the pressure of AGC is always larger than the working pressure of AC. Therefore, this property will be utilized to verify the AMEsim model for Type 3 IC HPS.

B. MODEL VERIFICATION

Figure 3 compares the dynamic properties (Output force-Displacement based on the excitation signal listed in Table 2 for No.1 and 2 testing signals) of Type 1 and 2 IC HPS based on the experimental data from Lin *et al.* [24], and those obtained through the established AMEsim model, as shown in Figure 2. It can be easily observed from Figure 3 that the AMEsim model can greatly catch the characteristic of the

TABLE 1. Parameters setting of the simulation.

Definition	Description	Value	Unit
A_1	Area of main chamber (MC)	3117	mm^2
A_2	Area of piston rod	1590	mm^2
A_3,	Area of annular chamber (AC)	1527	mm^2
A_4	Area of gas chamber (GC)	884	mm^2
A_5	Area of annular gas chamber (AG) of Type 3	1527	mm^2
D_{13}	diameter of the connection pipe	6	mm
L_{13}	length of the connection pipe	2.5	m
n_{12}	Number of orifices between the main chamber and piston rod oil chamber	10	
a_{12}	Area of orifice between the main chamber and piston rod oil chamber	3.10	mm^2
n_{13}	Number of orifices between the main chamber and annular chamber of Type 2	22	
a_{13}	Area of orifice between the main chamber and annular chamber of Type 2	1.70	mm^2
V_4	Maximum volume of gas chamber (GC)	249000	mm^3
V_5	Maximum volume of annular gas chamber (AG) (only in Type 3)	120000	mm^3
C_d	Flow coefficient	0.7	
n	Polytropic index	1.4	
h_0	Initial testing position of the two struts (compressed from the full-extended position)	73.8	mm
P_{40}	Pre-charge pressure in the gas chamber	0.44	MPa
P_{50}	Pre-charge pressure in the annular gas chamber (only in Type 3)	0.44	MPa

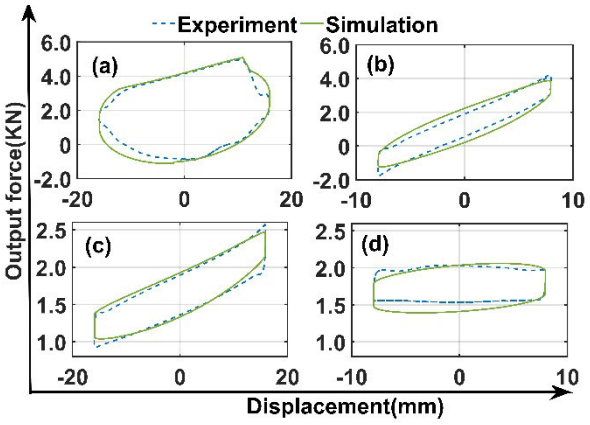

FIGURE 3. Comparison of the experimental data and simulation result. (a) Type 1 (No.1 testing signal in Table 2); (b) Type 1 (No.2 testing signal in Table 2); (c) Type 2 (No.1 testing signal in Table 2); (d) Type 2 (No.2 testing signal in Table 2).

experimental result. The main difference exists in No.2 testing signal for Type 2 IC HPS, which is mainly related to the fact that simple Coulomb damper model was utilized in the established AMEsim model and ignoring the inner effect of the friction, as mentioned before, and for Out-of-Phase excitation, the whole system is very sensitive to the pressure distribution, which is associated with the friction [24].

As mentioned above, the validity of Type 3 IC HPS AMEsim model will be verified through the dynamic properties comparison with those for Type 1 IC HPS under large initial charging pressure for AGC, as listed in Table 2. Figure 4(a) and (b) illustrate the simulation result of Output force-Displacement for both Type 1 and 3 IC HPS based on the No 1 and 2 test signals listed in Table 2. Perfect match can be found from Figure 4(a) and (b) for Type 1 and 3 IC HPS. One can also find from Figure 4(c) and (d) that under lower initial charging pressure for AGC of Type 3 IC HPS, the negative pressure working range of Type 3 IC HPS is significantly smaller than that for Type 1 IC HPS. However, big jump can be observed in the compression stoke for Type 3 IC HPS, which is mainly because of the stick of the added annular piston because of the "stop point", which will be discussed in detailed in the next part. From Figure 4, it can be found that as expected under large pre-charging initial pressure in AGC the dynamic properties of Type 3 IC HPS is similar to that for Type 1 HPS, and then the validity of the established AMEsim model for Type 3 IC HPS can also be verified.

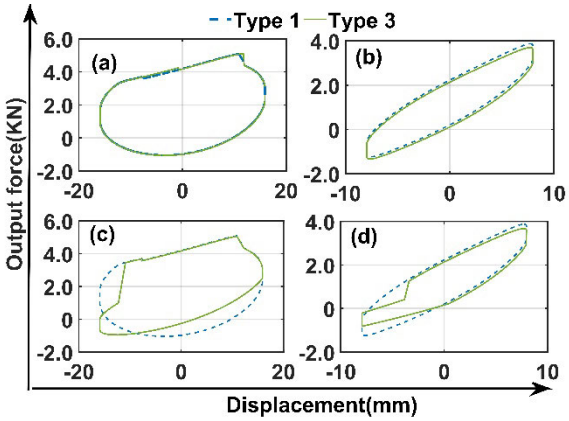

FIGURE 4. Comparison of the experimental data and simulation result: (a) No.1 testing signal in Table 2 (b) No.2 testing signal in Table 2 (c) No.3 testing signal in Table 2 (d) No.4 testing signal in Table 2.

Based on the above analysis, the validity of the established AMEsim models for Type 1, 2 and 3 IC HPS has been verified. In the next part, the detailed performance comparison and analysis will be presented.

IV. DISCUSSION

As the main purpose of this paper is to proposed one type of IC HPS, as shown in Figure 1(c), which can provide good stiffness properties comparing with Type 2 IC HPS under Out-of-Phase working condition, and greatly shorten the distortion working range comparing with the Type 1 IC HPS. Therefore, in this section the validity of the Type 3 IC HPS will be verified firstly, and it will be shown that Type 3 IC HPS has greater application potential comparing with the other types of IC HPS. And then the investigation of dynamic properties based on extensive excitation signals will be presented. Finally, the sensitive analysis of the most important

TABLE 2. Excitation signals for model verification.

Number	Frequency (Hz)	Amplitude (mm)	Phase	Pressure (GC)	Pressure (AGC)
1	2.0	15.92	In-phase	0.44Mpa	3.00Mpa
2	1.0	7.96	Out-of-phase	0.44Mpa	3.00Mpa
3	2.0	15.92	In-phase	0.44Mpa	1.50Mpa
4	1.0	7.96	Out-of-phase	0.44Mpa	1.50Mpa

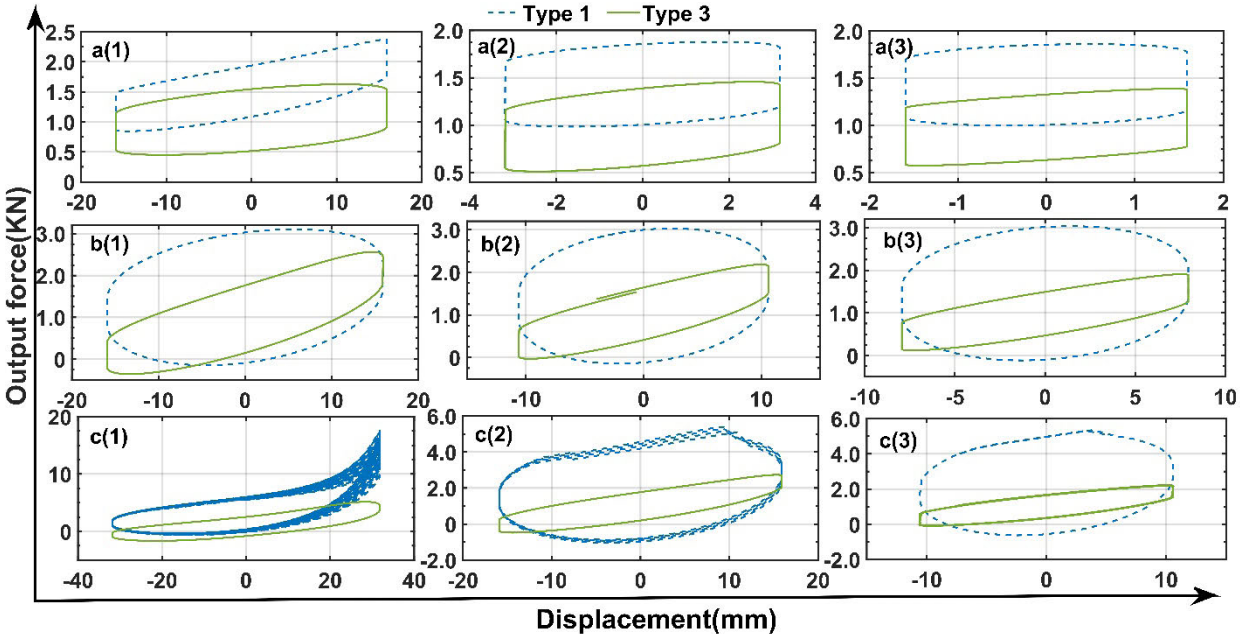

FIGURE 5. Dynamic properties (Output force-Excitation Displacement) comparison of Type 1 and Type 3 IC HPS with different testing signal listed in Table 3. Note: the number in figures is similar those listed in Table 3.

TABLE 3. The test signals for the dynamic performance comparison (In-phase test).

Number	Frequency (Hz)	Amplitude (mm)	Peak velocity (m/s)	Pressure (GC)	Pressure (AGC)
a(1)	0.1	15.92	0.01	0.44Mpa	0.44Mpa
a(2)	0.5	3.18		0.44Mpa	0.44Mpa
a(3)	1.0	1.59		0.44Mpa	0.44Mpa
b(1)	1.0	15.92	0.10	0.44Mpa	0.44Mpa
b(2)	1.5	10.61		0.44Mpa	0.44Mpa
b(3)	2.0	7.96		0.44Mpa	0.44Mpa
c(1)	1.0	31.83	0.20	0.44Mpa	0.44Mpa
c(2)	2.0	15.92		0.44Mpa	0.44Mpa
c(3)	2.5	12.74		0.44Mpa	0.44Mpa

design parameter, the initial charging pressure of AGC of Type 3, will be discussed in detailed.

A. COMPARING WITH TYPE 1 IC HPS

According to those presented by Lin *et al.* [24], one can easily find that for Type 1 IC HPS there are three phenomenon which may not be acceptable for practical application: (1) force distortion; (2) large negative pressure working range; (3) easily to be lock in Out-of-Phase working condition. The above phenomenon are all related to the non-continues of fluid flow, which is associated to the pressure distribution, and then the peak velocity. In the following subsection, the dynamic properties comparison between Type 1 and 3 HPS will be presented based on three kinds of excitation signals: In-Phase test, Out-of-Phase test and Random test.

1) IN-PHASE TEST

The comparison of dynamic performance (Output force-Excitation displacement) under harmonic excitation signals

of Type 1 and Type 3 IC HPS based on the established AMEsim models for In-Phase test has been illustrated in Figure 5, and all of the test signals have been summarized in.

Basically, it can be observed from Figure 5 that for Type 3 IC HPS (1) the maximum output force is smaller than that of Type 1, which is because of the fact that the added extra gas chamber will make the hydraulic system softer; (2) the condition of negative output force has been attenuated significantly comparing with Type 1 IC HPS, except at the end of the extension stroke (close to the maximum extension point) under large amplitude excitation signals (Figure 5 (b1)). This is mainly due to the fact that the inner influence of the friction of annular piston in the AMEsim model building in this paper has been neglected, so the oil in this system may more likely to push the annular piston to squeeze the volume of AGC (no resistance) rather than flow to the MC through the interconnection pipe (high resistance) at the end of extension stroke, which will lead to the pressure in AC greater than that in MC and then the condition of negative force occurs; (3) the condition of the output force disturbance vanishes.

From Figure 5, one can also found that (1) comparing Figure 5 (a), (b), and (c), with the increasing of the peak velocity, Type 3 IC HPS shows stable dynamic properties, but the Type 1 IC HPS not. This is mainly due to the block of hydraulic flow in the Type 1 IC HPS design between the connection pipes as discussed by Lin *et al.* [24]; (2) comparing Figure 5 (c) under the same peak velocity, with the increasing of the excitation amplitude, the Type 1 IC HPS shows significant force distortion, which is also due to the block of hydraulic flow between the connection pipes as discussed by Lin *et al.* [24], but Type 3 IC HPS shows very stable dynamic properties.

Furthermore, it should be noted from Figure 5 a(1), b(1) and c(2) that under the same excitation amplitude, the output force of Type 3 IC HPS in higher excitation frequency is larger than that in lower one, which is mainly due to the fact that the oil in compression stroke will push the floating piston to squeeze the gas in GC rather than passing through the interconnection pipe under higher peak velocity, which will lead to the increasing of the output force.

2) OUT-OF-PHASE TEST

The comparison of dynamic performance (Output force-Excitation displacement) under harmonic excitation signals of Type 1 and Type 3 IC HPS based on the established AMEsim models for Out-of-Phase test has been illustrated in Figure 6, which illustrate the dynamic properties of the right side HPS. Table 4 summarized all of the test signals.

One can easily find from Figure 6 that (1) Type 1 IC HPS shows large negative force working range from the end of the extension stroke and increasing with the increase of the excitation frequency. This is mainly due to the block of fluid flow in the connection pipes, as discussed by Lin *et al.* [24];

TABLE 4. The test signals for the dynamic performance comparison (Out-of-Phase test).

Number	Frequency (Hz)	Amplitude (mm)	Pressure (GC)	Pressure (AGC)
1	0.10	7.96	0.44Mpa	0.44Mpa
2	1.00	7.96	0.44Mpa	0.44Mpa
3	2.00	7.96	0.44Mpa	0.44Mpa

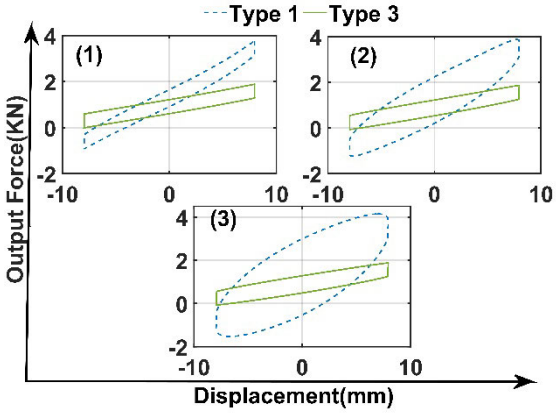

FIGURE 6. The comparison of Type 1 IC HPS and Type 3 IC HPS at Out-of-phase test. Note: the number in figures is similar those listed in Table 4.

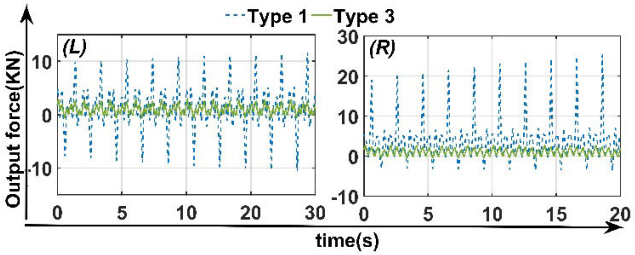

FIGURE 7. The comparison of Type 1 and Type 3 IC HPS at Random test.

(2) Comparing with Type 1 IC HPS, Type 3 IC HPS shows positive output force in the whole testing range and stable dynamic properties. Here, it should be noted that as mentioned in section III(*B*) the dynamic properties of Type 3 IC HPS can be modified by the initial charging pressure of AGC, and this point will be investigated in detailed in the Sub-section IV(*C*).

3) RANDOM TEST

Based on the analysis presented in the above two Subsections, one may be realized that under random types of excitation, Type 1 IC HPS may not work stable. In this section, simple combination of harmonic excitation, as shown in Equation. (26) and (27), will be utilized to test the dynamic properties of Type 1 and 3 IC HPS under random type of test signal.

Figure 7 illustrates the output force in time domain, from which one can easily realize that Type 1 IC HPS may not be

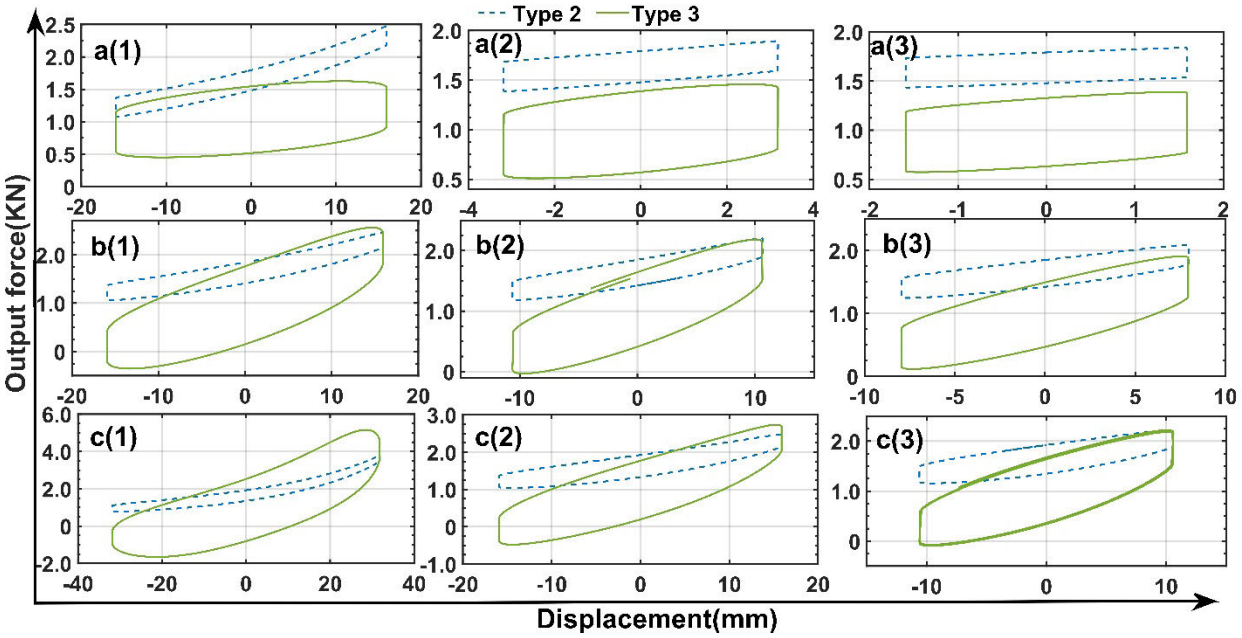

FIGURE 8. Dynamic properties (Output force-Excitation Displacement) comparison of Type 2 and Type 3 IC HPS with different testing signal listed in Table 3. Note: the number in figures is similar those listed in Table 3.

suitable for random type excitation in this kind of excitation condition.

$$x_L = 0.01\sin(2*pi*t) + 0.004\sin(2*pi*1.5*t) + 0.006\sin(2*pi*3*t) \quad (26)$$

$$x_R = 0.01\sin(2*pi*2*t) + 0.003\sin(2*pi*t) + 0.005\sin(2*pi*0.5*t) \quad (27)$$

Based on the above comparison, one can easily find that Type 3 IC HPS can overcome the drawback (distortion, negative force condition) of Type 1 IC HPS, and then is able to work in Random test signal, except that provide lower output force comparing with Type 1 IC HPS.

B. COMPARING WITH TYPE 2 IC HPS

Based on the investigation presented by Lin *et al.* [24], the main drawback for Type 2 IC HPS is the low stiffness in the Out-of-Phase test signal. Although, it can be improved through the modification of the dimension of the connection pipes and the orifice between the AC and MC. As mentioned before, Type 3 IC HPS will be designed to improve the stiffness in the Out-of-Phase condition comparing with those for Type 2 IC HPS. Therefore, in this section the comparison of dynamic properties of Type 2 and 3 IC HPS in the In-Phase and Out-of-Phase test will be presented.

1) IN-PHASE TEST

The typical testing signals for the In-Phase test are the same as those listed in Table 3. Figure 8 illustrated the dynamic properties comparison for the Type 2 and 3 IC HPS.

From Figure 8, one can easily find that (1) Comparing with Type 2 IC HPS, Type 3 can effectively improve the stiffness,

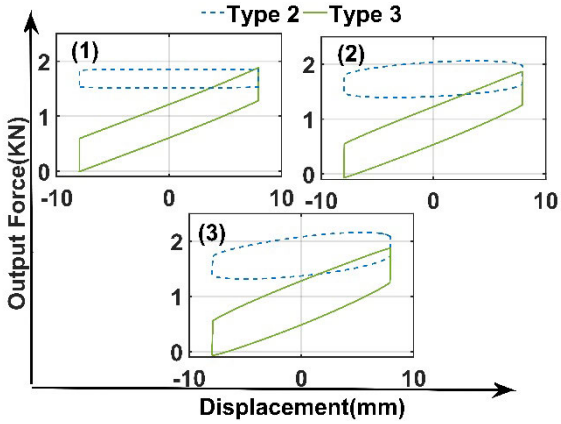

FIGURE 9. Comparison of output force of Type 2 IC HPS and Type 3 IC HPS at out-of-phase test. Note: the number in figures is similar those listed in Table 4.

and it will be increased with the increase of the peak velocity, except under low frequency and large amplitude excitation signals; (2) negative output force can be observed for Type 3 IC HPS, which is still mainly due to the block of the fluid flow between the connection pipes as discussed before and presented by Lin *et al.* [24]; (3) under low frequency and large amplitude excitation (low peal velocity, as illustrated in Figure 8 (a1)) test signal, the Type 2 IC HPS shows large stiffness properties comparing with Type 3 IC HPS,. This is mainly due to the fact that under low peak velocity, the hydraulic fluid can easily flow between the MC (R or L) and AC (L of R), and in this condition the maximum output force is directly related to the compression of gas chamber, as those presented by Lin *et al.* [24].

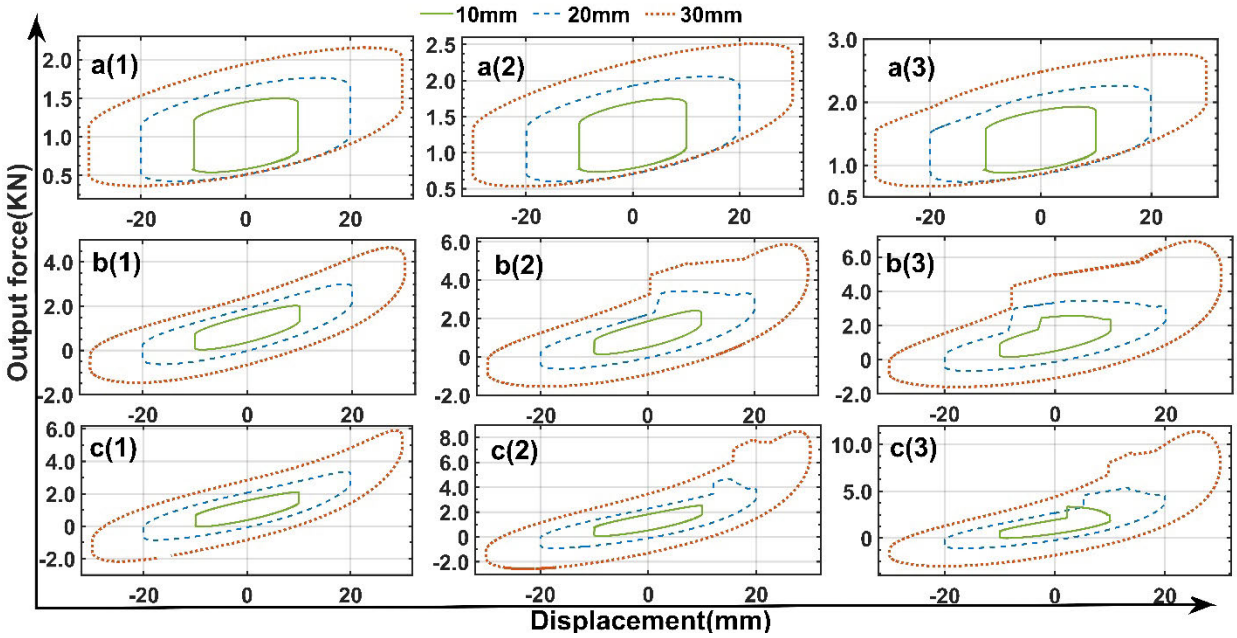

FIGURE 10. Simulation result of Type 3 IC HPS under different pre-charging pressure in AGC at In-Phase test. Note: the number in figures is similar those listed in Table 5.

TABLE 5. In-phase excitation (Pressure GC, 0.44Mpa).

Number	Frequency(Hz)	Amplitude(mm)	Pressure(AGC)	Pressure Ratio (AGC/GC)
a(1)	0.1	10/20/30	0.44Mpa	1.00
a(2)	0.1	10/20/30	0.60Mpa	1.36
a(3)	0.1	10/20/30	0.80Mpa	1.82
b(1)	1.0	10/20/30	0.44Mpa	1.00
b(2)	1.0	10/20/30	0.60Mpa	1.36
b(3)	1.0	10/20/30	0.80Mpa	1.82
c(1)	2.0	10/20/30	0.44Mpa	1.00
c(2)	2.0	10/20/30	0.60Mpa	1.36
c(3)	2.0	10/20/30	0.80Mpa	1.82

2) OUT-OF-PHASE TEST

The typical testing signals for the Out-of-Phase test are the same as those listed in Table 4. Figure 9 illustrated the dynamic properties comparison for the Type 2 and 3 IC HPS.

It can be found from Figure 9 that comparing with those for Type 2 IC HPS, Type 3 can effectively improve the stiffness under Out-of-Phase working condition, which is the main drawback for Type 2 IC HPS design as presented by Lin *et al.* [24].

Based on the above analysis, one can easily find the proposed novel IC HPS design (Type 3) can provide good stiffness properties comparing with Type 2 IC HPS under Out-of-Phase working condition, and greatly shorten the distortion working range comparing with the Type 1 IC HPS. For these kinds of IC HPS design, Lin *et al.* [24] already presented the influence of the dimension of the connection pipes and the orifice (Type 2) to the dynamic properties of the IC HPS. For the proposed the IC HPS design (Type 3), the initial charging pressure in AGC play the essential role, and then in the next Sub-section the investigation of that will be presented in detailed.

C. INFLUCENCE OF THE PRE-CHARGING PRESSURES IN AGC OF TYPE 3 IC HPS

Based on the above two parts of performance comparison between the proposed IC HPS (Type 3) with those for Type 1 and Type 2 IC HPS, and those presented in Section 3.2 for model verification, one can realized that the performance of Type 3 IC HPS is extremely sensitive to the pre-charging pressure of the add Annual Gas Chamber (AGC). Therefore, this sub-section will be focused on investigation of the influence of the pre-charging pressure of AGC under different working condition, which includes In-Phase excitation and Out-of-Phase excitations.

1) IN-PHASE TEST

Table 5 summarized the test signals adopted in this study. Figure 10 illustrated the simulation results between the excitation displacement and the output force for the test signals listed in Table 5.

It can be observed from Figure 10 that (1) under the same excitation signals, with the increasing of the Pressure Ratio, the output force will be increased; (2) with the increasing of

the Pressure Ratio, the output force will be easier to reach the negative force area and the phenomenon of force distortion occurs. This is because of the fact that with the increasing of the Pressure Ratio the AGC gradually loses its function as a buffer and the system will be close to Type 1 IC HPS; (3) under the same Pressure Ratio, with the increase of excitation frequency (peak velocity), the system will also be easier to reach the negative force working range and phenomenon of force distortion occur. It because that the function of AGC to be working as buffer is limited by the pre-charging pressure, and under the same Pressure Ratio, the fluid block condition will be easier to happen with the increase of excitation frequency (peak velocity), so the negative force and phenomenon of force distortion will be easier to occur.

It can also be found output force jumping points from Figure 10. These jumping points occur at the compression stroke, and it is related to the Pressure Ratio and the peak velocity. The main reason is that at the compression stroke the volume of the total Annual chamber (AGC and AC) will increase, and then the annular piston will touch the ''Stop point''. Therefore, (1) under low peak velocity, as illustrated in Figure 10 (a1) to (a3), the jumping will not happen, this is because of the fact that the effect of resistance between the connection pipes is small; (2) under the same set the excitation signal, the jumping points will be more easily to happen with the increase of Pressure Ratio, which will make the pressure in AGC is much higher than the system pressure in the compression working stroke, and then the annular piston will be easier to touch the ''Stop point''; (3) under the same Pressure Ratio, with the increase of the peak velocity, the jumping points will not show constant trend, as the whole system is directly related to the pressure distribution, which is directly associated with the resistance on friction of piston, orifices and the connection pipes, which will be investigated in the future research.

2) OUT-OF-PHASE TEST

Table 6 summarized the test signals adopted in this study for the Out-of-Phase test. Figure 11 illustrated the simulation results between the excitation displacement and the output force for the test signals listed in Table 6

TABLE 6. Out-of-phase (Pressure GC, 0.44Mpa).

Number	Frequency(Hz)	Amplitude(mm)	Pressure(AGC) (Mpa)
1	0.1	7.96	0.44/0.6/0.8
2	1	7.96	0.44/0.6/0.8
3	2	7.96	0.44/0.6/0.8

Actually, very close conclusion as presented in Figure 10, can be observed from Figure 11. With the increase of Pressure Ratio, the output force increases, and finally the system will be similar to Type 1 IC HPS, as discussed in Sub-section III(*B*).

Considering the above investigation and analysis applied on the Type 3 IC HPS, one can realize that the dynamic

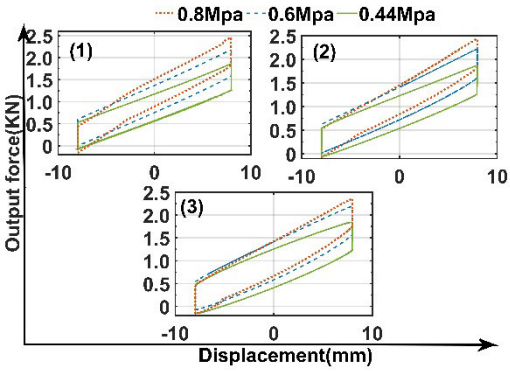

FIGURE 11. Simulation result of Type 3 IC HPS under different pre-charging pressure in AGC at out-of-phase test.

properties of Type 3 I HPS can be easily modified trough the pre-charging pressure in the AGC, and its combination with the orifices between the MC and AC, and the size (length and dimension) of the connection pipes. Therefore, through property calibration, the proposed IC HPS design can meet different practical requirement.

V. CONCLUSION

One kind of Inter-Connected Hydro-Pneumatic Struts (IC HPS), which is designed based on the developed double-gas-chamber compacted Hydro-Pneumatic Struts (HPS) integrating double inner gas chambers, has been proposed in this research. Based on extensive investigation on the dynamic properties of the proposed IC HPS, it has been shown that comparing with the traditional IC HPS designs (Type 1 and 2 IC HPS in Figure 1(a) and (b)), the proposed IC HPS (Type 3 IC HPS in Figure 1(c)) can provide good stiffness properties comparing with Type 2 IC HPS under Out-of-Phase working condition, and greatly shorten the distortion working range, and negative force range comparing with the Type 1 IC HPS.

Considering that the dynamic properties of the proposed IC HPS is very sensitive to the essential design parameter, the initial charging pressure of the Annular Gas Chamber (AGC), extensive design parameter sensitivity analysis has been conducted on this essential design parameter. The result suggested that the dynamic of the proposed IC HPS can be modified in large working range through the pre-charging pressure in AGC.

Overall, this research presented in this paper suggested that the proposed IC HPS has more application potential comparing with other types of IC HPS. Here, it should be noted that (1) as the main purpose of this research paper is to propose and verify the validity of the proposed IC HPS, and for the seeking of clear expression, some important parameters, such as the inner effect of the friction in the floating and annular pistons, and the friction models, have been simplified, which will be one of the future research topics; (2) although the model validation is based on part of experimental data, to obtain more accuracy dynamic model, especially the friction model in the system, completed experimental set-up will be conducted in the future work; (3) other

effect of design parameters, such as the dimension of the connection pipes and orifices between the MC and RC, will also be investigated based on the design experimental set-up in the future works; (4) this paper utilizes the typical test signals (In-Phase, Out-of-Phase and random test signals) to evaluate the performance of IC HPS based on force excitation signals, which is popularly utilized in the first step design analysis for IC HPS, and the result shows superior performance of the proposed IC HPS comparing with those presented by Wu [15] and Lin et al [24]; Here, it should be noted that the whole performance analysis should also include the base excitation test, which will be future research topic.

REFERENCES

[1] E. H. Law, "Theory of ground vehicles (second edition)," *J. Terramechanics*, vol. 31, no. 6, pp. 415–416, 1994.
[2] K. Choi, J. Oh, H.-S. Kim, H.-W. Han, J.-H. Park, G.-H. Lee, J. Seo, and Y.-J. Park, "Experimental study on the dynamic characteristics of hydro-pneumatic semi-active suspensions for agricultural tractor cabins," *Appl. Sci.*, vol. 10, no. 24, p. 8992, Dec. 2020.
[3] M. C. Smith and G. W. Walker, "Interconnected vehicle suspension," *Inst. Mech. Eng., D, J. Automobile Eng.*, vol. 219, no. 3, pp. 295–307, Mar. 2005.
[4] H. Li, Y. Wu, and M. Chen, "Adaptive fault-tolerant tracking control for discrete-time multiagent systems via reinforcement learning algorithm," *IEEE Trans. Cybern.*, vol. 51, no. 3, pp. 1163–1174, Mar. 2021.
[5] H. Liang, G. Liu, T. Huang, H.-K. Lam, and B. Wang, "Cooperative fault-tolerant control for networks of stochastic nonlinear systems with nondifferential saturation nonlinearity," *IEEE Trans. Syst., Man, Cybern. Syst.*, early access, Sep. 18, 2020, doi: 10.1109/TSMC.2020.3020188.
[6] K. Mei, L. Ma, R. He, and S. Ding, "Finite-time controller design of multiple integrator nonlinear systems with input saturation," *Appl. Math. Comput.*, vol. 372, May 2020, Art. no. 124986.
[7] R. N. Jazar, "Steering dynamics," in *Vehicle Dynamics*. New York, NY, USA: Springer, 2014, pp. 387–495.
[8] N. Zhang, W. A. Smith, and J. Jeyakumaran, "Hydraulically interconnected vehicle suspension: Background and modelling," *Vehicle Syst. Dyn.*, vol. 48, no. 1, pp. 17–40, Jan. 2010.
[9] G. Xu, N. Zhang, and H. M. Roser, "Roll and pitch independently tuned interconnected suspension: Modelling and dynamic analysis," *Vehicle Syst. Dyn.*, vol. 53, no. 12, pp. 1830–1849, Dec. 2015.
[10] D. Cebon, *Handbook of Vehicle-Road Interaction*. Lisse, Holland: Swets Zeitlinger, 1999.
[11] W. A. Smith, N. Zhang, and W. Hu, "Hydraulically interconnected vehicle suspension: Handling performance," *Vehicle Syst. Dyn.*, vol. 49, nos. 1–2, pp. 87–106, Feb. 2011.
[12] J. Wei, D. Yi, X. Bo, C. Guangyu, and Z. Dean, "Adaptive variable parameter impedance control for apple harvesting robot compliant picking," *Complexity*, vol. 2020, pp. 1–15, Apr. 2020.
[13] P. Du, Y. Pan, H. Li, and H. Lam, "Nonsingular finite-time event-triggered fuzzy control for large-scale nonlinear systems," *IEEE Trans. Fuzzy Syst.*, early access, May 6, 2020, doi: 10.1109/TFUZZ.2020.2992632.
[14] F. Ding, N. Zhang, J. Liu, and X. Han, "Dynamics analysis and design methodology of roll-resistant hydraulically interconnected suspensions for tri-axle straight trucks," *J. Franklin Inst.*, vol. 353, no. 17, pp. 4620–4651, Nov. 2016.
[15] L. Wu, "Analysis of hydro-pneumatic interconnected suspension struts in the roll plane vehicle model," M.S. thesis, Dept. Mech. Ind. Eng., Concordia Univ., Montreal, QC, Canada, 2003.
[16] D. Cao, S. Rakheja, and C. Y. Su, "Dynamic analyses of heavy vehicle with pitch-interconnected suspensions," *Int. J. Heavy Veh. Syst.*, vol. 15, no. 4, pp. 272–308, Jan. 2008.
[17] D. Cao, S. Rakheja, and C. Y. Su, "Dynamic analyses of roll plane interconnected hydro-pneumatic suspension systems," *Int. J. Vehicle Des.*, vol. 47, no. 4, pp. 51–80, Jan. 2008.
[18] D. Cao, S. Rakheja, and C.-Y. Su, "Roll- and pitch-plane-coupled hydro-pneumatic suspension. Part 2: Dynamic response analyses," *Vehicle Syst. Dyn.*, vol. 48, no. 4, pp. 507–528, Apr. 2010.
[19] D. Cao, "Theoretical analyses of roll-and pitch-coupled hydro-pneumatic strut suspensions," Ph.D. dissertation, Dept. Mech. Ind. Eng., Concordia Univ., Montreal, QC, Canada, 2008.
[20] K. Guo, Y. Chen, Y. Yang, Y. Zhuang, and Y. Jia, "Modeling and simulation of a hydro-pneumatic spring based on internal characteristics," in *Proc. 2nd Int. Conf. Mechanic Autom. Control Eng.*, Inner Mongolia, China, Jul. 2011, pp. 5910–5915.
[21] N. Jiao, J. Guo, and S. Liu, "Hydro-pneumatic suspension system hybrid reliability modeling considering the temperature influence," *IEEE Access*, vol. 5, pp. 19144–19153, 2017.
[22] Z. Zhang, S. Cao, and C. Ruan, "Statistical linearization analysis of a hydropneumatic suspension system with nonlinearity," *IEEE Access*, vol. 6, pp. 73760–73773, 2018.
[23] D. Lin, F. Yang, D. Gong, and S. Rakheja, "Design and experimental modeling of a compact hydro-pneumatic suspension strut," *Nonlinear Dyn.*, vol. 100, no. 4, pp. 3307–3320, Jun. 2020.
[24] D. Lin, F. Yang, D. Gong, F. Zhao, X. Luo, R. Li, and Z. Lin, "Experimental investigation of two types interconnected hydro-pneumatic struts," *IEEE Access*, vol. 7, pp. 100626–100637, 2019.

RUIHONG LI received the B.E. degree (Hons.) in mechanical engineering from Huaqiao University, Xiamen, China, in 2018, where he is currently pursuing the master's degree with the College of Mechanical Engineering and Automation. His research interests include vibration control and vehicle dampers.

FAN YANG received the B.E. degree (Hons.) in aerospace engineering from the Civil Aviation University of China, in 1996, and the M.S. and Ph.D. degrees in mechanical engineering from Concordia University, Montreal, QC, Canada, in 2004 and 2008, respectively. He was a Postdoctoral Research Fellow and a Research Associate with Concordia University, from 2009 to 2011, and he was appointed as an Associate Professor with the South China University of Technology. He is currently with the College of Mechanical Engineering and Automation, Huaqiao University, Xiamen, China, where he has been a Professor. His research interests include mechatronics, vibration control, and the application of smart material actuators and dampers.

DEZHAO LIN received the B.E. degree (Hons.) in mechanical engineering from Huaqiao University, Xiamen, China, in 2017, where he is currently pursuing the master's degree with the College of Mechanical Engineering and Automation. His research interests include vibration control and vehicle suspension.

CHENGHONG LI received the B.E. degree (Hons.) in mechanical engineering from Nanchang Institute of Technology, in 2019. He is currently pursuing the master's degree with the College of Mechanical Engineering and Automation, Huaqiao University, Xiamen, China. His research interests include mechatronics, vibration control, and smart materials.

HONGWEI CHEN received the B.E. degree (Hons.) in mechanical engineering from the Tianjin University of Technology, Tianjin, China, in 2019. He is currently pursuing the M.S. degree with the College of Mechanical Engineering and Automation, Huaqiao University, Xiamen, China. His research interests include MRE and the performance medical devices.

WENBO QIAN received the B.E. degree (Hons.) in mechanical engineering from Huaqiao University, Xiamen, China, in 2019, where he is currently pursuing the master's degree with the College of Mechanical Engineering and Automation. His research interests include vibration control and smart materials.

SHENG JIA received the B.E. degree (Hons.) in mechanical engineering from Huaqiao University, Xiamen, China, in 2019, where he is currently pursuing the master's degree with the College of Mechanical Engineering and Automation. His research interests include human engineering and hand-transmitted vibration.

FENG ZHAO received the B.E. degree in power mechanical engineering from the University of Shanghai for Science and Technology, China, in 1986, and the M.S. degree in mechanical engineering from Concordia University, Montreal, QC, Canada, in 1999. He is currently a Senior Research Fellow with the College of Mechanical Engineering and Automation, Huaqiao University, Xiamen, China. His research interests include mechatronics, robotic control, and artificial intelligence.